A three-spectrum method for accurate calibration of bi-plate zero-order retarder

Zhigang Han (韩志刚)[1,2,3], Zhi Xu (徐 治)[1,2*], and Lei Chen (陈 磊)[3]

[1] *Department of Chemistry and Biochemistry, University of Missouri-St.Louis, St. Louis, MO 63121, USA*

[2] *Center for NanoScience, University of Missouri-St.Louis, St. Louis, MO 63121, USA*

[3] *School of Electronic and Optical Engineering, Nanjing University of Science and Technology, Nanjing 210094, China*

[*] *Corresponding author: zhixu@umsl.edu*

Received December 12, 2013; accepted January 15, 2014; posted online February 28, 2014

A new spectroscopic method is proposed for the characterization of optical zero-order retarders. It is demonstrated that the retardance as well as the variation of the effective fast axis of a bi-plate zero-order quarter retarder (633 nm) can be obtained with high accuracy in a broadband wavelength range by taking spectra at only three independent angular orientations of the retarder. The calibration results excellently agree with theoretical models, indicating the new method could be used as a simple and reliable way for efficient self-spectral-calibration of optical zero-order retarders.

OCIS codes: 120.2130, 120.3940, 300.6170.

doi: 10.3788/COL201412.031202.

Zero-order retarders, manufactured by laminating a polymer film between two optical windows[1] or by assembling two or more multi-order retarders together[2,3], are widely used in polarimeters and ellipsometers[4−7]. Knowing characteristics of the retarder in a broadband wavelength range, including the retardance and variation of the orientation of the effective fast axis, is vital for the accuracy of spectroscopic polarimeters and ellipsometers. A multi-order retarder can be spectral-calibrated in a polarizer-retarder-analyzer (PRA) setup depicted by Fig. 1, through Fourier analysis or extreme analysis of a polarization interference spectrum[8−10]. However, for a zero-order retarder, the spectrum only presents low-frequency variation. The Fourier analysis and extreme analysis are inaccurate to characterize the zero-order retarder. Lin *et al.*[11] demonstrated that an elliptical retarder can be calibrated at a single wavelength through six intensity values. The methods can be extended to the spectral domain. Under the method, rotations are needed for both the polarizer and analyzer. Thus, polarization independent light source and spectrometer are required for the spectral-calibration with Lin's method[7].

Previous studies[1,7,12−14] indicate spectral-calibration of the zero-order retarder can be achieved by the rotating sample methods without the requirement of the polarization independent light source and spectrometer. Under the rotating sample methods, spectroscopic measurements are taken at several fast axis orientations using a double-pass setup with only two polarization optical components[1] or using the PRA setup[12−14]. The retardance and variation of the orientation of the effective fast axis can be extracted either by fitting the detected signals to a sinusoidal function[1] or from the Fourier frequency components of the detected signals[12]. The variation of the orientation of the effective fast axis can also be determined from the minimum of the detected signals at different wavelengths[13,14].

As shown by Fig. 1, a bi-plate zero-order retarder consists of two multi-order retarders, R_1 and R_2. Ideally, the fast axis of R_1 is aligned parallel to the slow axis of R_2. In reality, however, there is an alignment error between the two axes, which causes the wavelength dependent change in the orientation of the effective fast axis of the retarder[12−14].

In this letter, it is demonstrated that both the retardance and variation in the effective fast axis orientation of a bi-plate zero-order retarder can be accurately determined by taking spectroscopic measurements at three independent orientations of the effective fast axis using the PRA experimental setup depicted by Fig. 1.

In a measurement employing the PRA setup depicted by Fig. 1, the light from the light source (L), after passing through the polarizer (P), the bi-plate zero-order retarder (R), and the analyzer (A), is collected by the spectrometer (S). The spectroscopic signal can be expressed by[12,15,16]

$$S(\lambda) = Q(\lambda)\Big\{\cos^2\gamma - \sin 2\alpha(\lambda)\sin 2\left[\alpha(\lambda)-\gamma\right] \cdot \sin^2\frac{\delta(\lambda)}{2}\Big\}, \tag{1}$$

where $Q(\lambda)$ is the wavelength dependent coefficient accounting for emission spectrum of the light source, the optical transmissions of the polarizer (P), the retarder (R) and the analyzer (A), and the grating efficiency and detector response of the spectrometer (S); γ represents the angle between the polarization axis of the analyzer and that of the polarizer, $\alpha(\lambda)$ is the orientation angle, i.e., the angle between the effective fast axis of the retarder and the polarization axis of the polarizer, $\delta(\lambda)$ is the phase retardance of the bi-plate retarder. $\delta(\lambda)$ can be expressed by[15]

$$\delta(\lambda) = 2\pi\Delta n(\lambda)\Delta d/\lambda, \tag{2a}$$

where $\Delta n(\lambda)$ is birefringence dispersion of the retarder, and Δd is the effective thickness.

In the PRA setup shown in Fig. 1, the retarder R is typically mounted on a rotation stage, and the orienta-

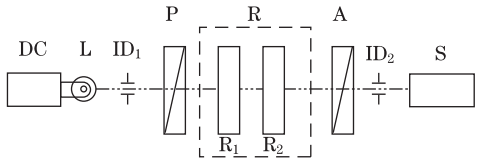

Fig. 1. Experimental layout for the spectral-calibration of the bi-plate retarder. DC: DC power supply, L: light source, ID_1-ID_2: iris diaphragms, P: polarizer, R: bi-plate retarder, R_1-R_2: multi-order retarders, A: analyzer, S: multi-channel grating spectrometer.

tion angle $\alpha(\lambda)$ can be expressed by

$$\alpha(\lambda) = \theta + \overline{\alpha_0} + \kappa(\lambda), \tag{2b}$$

where θ is the detection angle, i.e., the angular reading from the rotation stage, $\overline{\alpha_0}$ is the average initial orientation angle at $\theta = 0°$, and $\kappa(\lambda)$ is the variation of effective fast axis and is an intrinsic property of the retarder. The sum, $\alpha_0(\lambda) = \overline{\alpha_0} + \kappa(\lambda)$, is the initial orientation of the effective fast axis when $\theta = 0°$.

Eq. (1) can be rewritten as

$$S(\lambda) = A(\lambda)\left\{1 + M(\lambda)\cos\left[4\theta + 4\alpha_0(\lambda) - 2\gamma\right]\right\}. \tag{3}$$

In Eq. (3), $A(\lambda)$ and $M(\lambda)$ are the baseline and modulation at each wavelength[17], expressed by

$$A(\lambda) = \frac{Q(\lambda)}{2}\left[2\cos^2\frac{\delta(\lambda)}{2}\cos^2\gamma + \sin^2\frac{\delta(\lambda)}{2}\right], \tag{4a}$$

$$M(\lambda) = \frac{\tan^2\frac{\delta(\lambda)}{2}}{2\cos^2\gamma + \tan^2\frac{\delta(\lambda)}{2}}. \tag{4b}$$

Based on Eq. (3), $M(\lambda)$ and $\alpha_0(\lambda)$ can be retrieved from the spectra $S(\lambda)$ taken at three independent detection angles θ for a given $\gamma(\gamma \neq 90°)$. In this letter, three detection angles, $\theta_0 = 0°$, $\theta_1 = -22.5°$ and $\theta_2 = 22.5°$ are chosen for computational convenience. The sign of the detection angle θ is negative if the retarder is rotated clockwise when facing the light leaving the PRA setup shown in Fig. 1, and the sign of the detection angle θ is positive if the retarder is rotated counterclockwise when facing the light leaving the PRA setup shown in Fig. 1.

Under these conditions, $M(\lambda)$, $\alpha_0(\lambda)$ and $\delta(\lambda)$ can be determined using a three-step phase shifting technique[18]:

$$M(\lambda) = \frac{\sqrt{2\left[S_0(\lambda) - S_1(\lambda)\right]^2 + 2\left[S_0(\lambda) - S_2(\lambda)\right]^2}}{S_1(\lambda) + S_2(\lambda)}, \tag{5a}$$

$$\delta(\lambda) = 2\arctan\left[\sqrt{\frac{2M(\lambda)}{1 - M(\lambda)}}\cos\gamma\right], \gamma \neq 90°, \tag{5b}$$

$$\alpha_0(\lambda) = \frac{1}{4}\arctan\left[\frac{S_1(\lambda) - S_2(\lambda)}{2S_0(\lambda) - S_1(\lambda) - S_2(\lambda)}\right] + \frac{\gamma}{2}. \tag{5c}$$

In the experimental layout shown by Fig. 1, a modified fiber optic illuminator (L, 190-1, Dolan Jenner, USA), powered by a DC power supply (GPR-1811HD), was used as the light source. Two iris diaphragms (ID 1.0, Newport, USA), each adjusted to 2 mm in diameter, were placed 50 cm apart in the light path to limit the beam divergence. Two dichroic sheet polarizers (03FPG003, 380 to 780 nm, CVI Melles Griot, USA) were employed as both the polarizer and the analyzer. The polarizer and the analyzer were both mounted on the polarizer holders (07HPR221, CVI Melles Griot, USA) with 1° angular interval. The polarization axis of the analyzer was aligned parallel to that of the polarizer ($\gamma = 0°$). A quartz bi-plate retarder (WPQ05M-633, Thorlabs, USA) was investigated. The retarder was manufactured as a zero-order quarter retarder at 633 nm with 1.2^o uncertainty in its retardance at 633 nm. The nominal thicknesses of the two multi-order retarders were 996.1 and 978.6 μm, leading to an effective thickness of $\Delta d = 17.5$ μm. The retarder was mounted on a motorized rotation stage (495A, Newport, USA) with 0.001° angular resolution. The spectra were taken by a multi-channel grating spectrometer (USB 4000, Ocean optics, USA) with 0.21-nm data interval and 4-nm spectral resolution. The integration time was 3.8 ms, and each spectrum was averaged for 1000 times to achieve better signal-to-noise (S/N) ratio. The dark spectrum was taken under the same condition with the light beam blocked before the polarizer. All data were collected at room temperature (24±1 °C).

Figure 2 shows three spectra, $S_0(\lambda)$, $S_1(\lambda)$, and $S_2(\lambda)$, taken from 550 to 700 nm at the three detection angles: $\theta_0 = 0°$, $\theta_1 = -22.5°$ and $\theta_2 = 22.5°$, with dark spectrum subtracted. The lower intensity signal near 550 nm in each spectrum is mainly caused by low light source power and low grating efficiency of the spectrometer in the wavelength region.

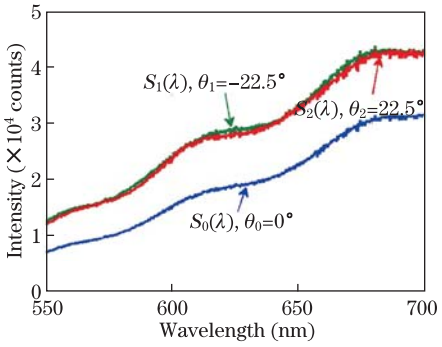

Fig. 2. (Color online) Three spectra, $S_0(\lambda)$, $S_1(\lambda)$, and $S_2(\lambda)$, taken at the detection angles $\theta_0 = 0°$, $\theta_1 = -22.5°$, and $\theta_2 = 22.5°$.

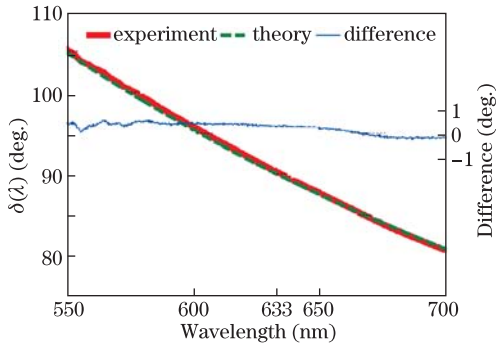

Fig. 3. (Color online) Experimental and theoretical results of retarance (left vertical scale) and their differences (right vertical scale).

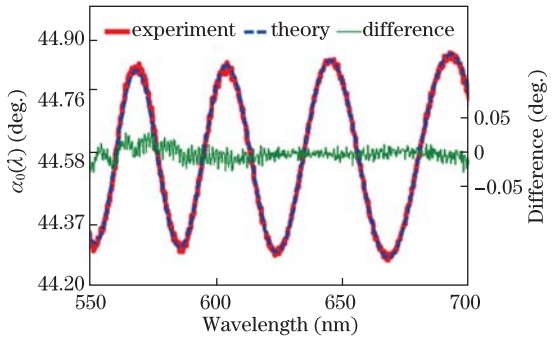

Fig. 4. (Color online) Experimental and theoretical results of the initial orientations of fast axes (left vertical scale) and their differences (right vertical scale).

Figur 3 shows the wavelength dependent retardance, $\delta(\lambda)$, obtained from the experimental results (heavy solid line) and that from theoretical calculation (dashed line), as well as their difference (fine solid line in the middle of the figure). The experimental retardance is obtained according to Eqs. (5b) using the three spectra shown in Fig. 2. The retardance decreases monotonically with wavelength, from 105.2° at 550 nm to 80.9° at 700 nm. At 633 nm, the experimental value is 90.4°. The theoretical values of $\delta(\lambda)$ are calculated according to Eq. (2a), with the effective thickness $\Delta d = 17.5$ μm and the values of birefringence dispersion from Ghosh's study[17]. The average value and the standard deviation of difference between the two are 0.19° and 0.22°, respectively, demonstrating excellent accuracy of the new method in determination of retardance $\delta(\lambda)$ of bi-plate zero-order retarder.

Figure 4 shows the experimental results (heavy solid line) and theoretical calculations (dashed line) of orientation angle $\alpha_0(\lambda)$. The experimental results are obtained according to Eq. (5c) using the three spectra shown in Fig. 2. The orientation of the effective fast axis of the retarder oscillates between 44.28° and 44.87° (0.59° peak-to-valley), with an average of $\overline{\alpha_0} = 44.58°$. The theoretical values are obtained using Eq. (6), based upon previous studies of elliptical polarization eigenstates[13,19]:

$$\alpha_0(\lambda) = \beta + \frac{1}{2}\arctan \cdot \left\{ \frac{\sin 2\varphi \tan\left[\frac{\pi\Delta n(\lambda)(d_1-\Delta d)}{\lambda}\right]}{\cos 2\varphi \tan\left[\frac{\pi\Delta n(\lambda)(d_1-\Delta d)}{\lambda}\right] - \tan\left[\frac{\pi\Delta n(\lambda) d_1}{\lambda}\right]} \right\}. \quad (6)$$

In Eq. (6), φ is the angle between the fast axis of R_1 and the slow axis of R_2, i.e., the alignment error, d_1 is the thicknesses of the R_1, Δd is the effective thickness of the bi-plate retarder, and β is the angle between the fast axis of R_1 and the polarization axis of the polarizer. Three independent parameters β, φ, d_1 are used to fit the experimental results using Levenberg-Marquardt curve fitting procedure[20]. Initial values of the parameters are set as $\beta = 44.58°$, $\varphi = 0°$, and $d_1 = 996.1$ μm. The fitted result are $\beta = 44.37°$, $\varphi = 0.39°$, and $d_1 = 989.9$ μm. The fine solid curve in middle of the figure shows the difference between the experimental results and the theoretical modeling. The average of the difference is close to zero ($<10^{-4}$), and the standard deviation is 0.0092°, showing excellent agreement between the two.

The alignment error in γ, the angle between the polarization axis of the analyzer and that of the polarizer, has negligible effect on the experimental results. For example, assuming that the actual value of γ is 1°, instead of 0°, the difference in the experimental value of the retardance at 633 nm is only 0.0087°, according to Eq. (5a). The same misalignment of 1° in γ causes a vertical shift of 0.5° in the orientation angle $\alpha_0(\lambda)$, according to Eq. (5c), and has no effect on the variation of the effective fast axis of the retarder, $\kappa(\lambda)$.

In conclusion, a new spectroscopic method has been demonstrated for the accurate calibration of the bi-plate zero-order retarder by taking spectroscopic measurements at only three independent detection angles. Although the new method has been demonstrated for the calibration of bi-plate zero-order retarders, it could also be used for the calibration of other similar or more complicated retarder systems.

The authors would like to thank Mr. Tor Holste of Thorlabs Inc. for consultations on technical details and specifications of the bi-plate retarder used in this study. Zhi-gang Han would like to appreciate the financial support from China Scholarship Council (No. 2011684023).

References

1. J. Zallat, M. Torzynski, and A. Lallement, Opt. Lett. **37,** 401 (2012).
2. P. Marsik and J. Humlicek, Phys. Stat. Sol. (c) **5,** 1064 (2008).
3. J. L. Vilas, L. M. Sanchez-Brea, and E. Bernabeu, Appl. Opt. **52,** 1892 (2013).
4. X. Zhang, Appl. Opt. **52,** 7078 (2013).
5. S. Cao, Y. Bu, X. Wang, S. Li, F. Tang, and Z. Li, Acta Opt. Sin. **33,** 0612010 (2013).
6. X. Meng, J. Li, D. Liu, and R. Zhu, Opt. Lett. **38,** 778 (2013).
7. L. Watkins and M. Derbois, Appl. Opt. **51,** 5060 (2012).
8. W. Feng, L. Lin, L. Chen, H. Zhu, R. Li, and Z. Xu, Chin. Opt. Lett. **4,** 705 (2006).
9. P. Hlubina and D. Ciprian, Opt. Lett. **35,** 1566 (2010).
10. W. Peng, L. Xi, X. Weng, Z. Xia, D. Zhao, and X. Zhang, Chin. Opt. Lett. **11,** 080604 (2013).
11. P. Lin, C. Han, and Y. Chao, Opt. Commum. **281,** 3403 (2008).
12. D. Chnault and R. Chipman, Appl. Opt. **32,** 3513 (1993).
13. B. Boulbry, B. Bousquet, B. Le Jeune, Y. Guern, and J. Lotrian, Opt. Express **9,** 225 (2001).
14. B. Boulbry, B. Jeune, F. Pellen, J. Cariou, and J. Lotrian, J. Phys D: Appl. Phys. **35,** 2508 (2002).
15. M. Born and E. Wolf, *Principles of Optics* (Cambridge, London, 2003).
16. J. Wang, L. Chen, B. Li, L. Shi, and T. Luo, Opt. Laser Eng. **48,** 698 (2010).
17. G. Ghosh, Opt. Commun. **163,** 95 (1999).
18. D. Malacara, *Optical Shop Testing* (Wiley-Interscience, Hoboken, New Jersey, 2007).
19. I. Scierski and F. Ratajczyk, Optik **68,** 121 (1984).
20. Curve fitting toolbox for use with MATLAB (Mathworks, 20).